

Seasonal prediction of monsoon rainfall in three Asian river basins: the importance of snow cover on the Tibetan Plateau

W. W. Immerzeel^{a,b*} and M. F. P. Bierkens^{b,c}

^a *FutureWater, Costerweg 1G, 6702 AA Wageningen, The Netherlands*

^b *Department of Physical Geography, Utrecht University, PO Box 80115, Utrecht, The Netherlands*

^c *Deltares, PO Box 80015, Utrecht, The Netherlands*

ABSTRACT: Empirical and numerical studies aiming at predicting inter-annual monsoon variability have thus far shown limited predictive capability. In this study, we develop a spatially explicit seasonal prediction methodology for south-west Asian monsoon (SWM) rainfall in the river basins of the Indus, Brahmaputra and Ganges, using multiple regression linear models in combination with satellite-derived snow cover. We show that the use of recent time series of remotely sensed snow cover, in combination with indices of global ocean and atmospheric modes (ENSO, NAO), can predict average monsoon precipitation with reasonable accuracy and with greater accuracy in specific regions. Maps of the relative contribution of predictor variables to the regression model show that the spring snow cover on the Tibetan plateau is the most important predictor of monsoon precipitation, especially in inland regions. Copyright © 2009 Royal Meteorological Society

KEY WORDS monsoon; ENSO; NAO; snow; TRMM; Tibetan Plateau

Received 30 January 2009; Revised 1 September 2009; Accepted 1 September 2009

1. Introduction

The Asian monsoon is a spectacular phenomenon in the earth's climate system and billions of people benefit or suffer from its seasonal rains. The monsoon is highly complex and is the resultant of the seasonal progression of earth's rotation and solar radiation, large-scale ocean–atmospheric modes such as the El Niño Southern Oscillation (ENSO) and the complex thermo-dynamic interaction between the atmosphere and the land surface (Wang, 2006).

The relation between the monsoon and ENSO has been explored in numerous studies, and a review is provided by Webster *et al.* (1998). The general consensus is that, during El Niño years, anomalous subsidence suppresses convection over South Asia and this generally results in a weaker monsoon (Kumar *et al.*, 1999). Besides ENSO, there is also emerging evidence that the Northern Atlantic Oscillation (NAO) is linked to the Asian summer monsoon (Yang *et al.*, 2004).

The land-ocean thermal contrast is another primary driver for the Asian monsoon (Li and Yanai, 1996; Liu and Yanai, 2001). A crucial factor is the snow cover on the Tibetan plateau that exerts a great influence on the thermodynamic balance, and subsequently on

tropospheric temperatures due to the plateau's high elevation. Over a century ago, Blanford (1884) already identified an inverse relationship between Himalayan snow cover in winter and spring, and the following summer monsoon. This study inspired numerous further studies of monsoon variability and snow interaction (Hahn and Shukla, 1976; Bamzai and Shukla, 1999; Robock *et al.*, 2003; Shaman *et al.*, 2005; Shaman and Tziperman, 2005). The influence of snow on the temperature gradient is explained by the following reinforcing physical processes. An increased snow pack yields a higher albedo, leaving less solar radiation available for generating sensible heat fluxes. Of the remaining energy, a substantial part is used for sublimation of snow. This process eventually leaves a wet surface that causes a large portion of solar energy to satisfy the latent heat demand associated with high evaporation rates.

Empirical and numerical studies aiming at predicting inter-annual monsoon variability have thus far demonstrated limited success. Many of the empirical studies use ENSO and/or NAO indicators as major predictors with moderate skill (Shukla and Paolino, 1983; Ropelewski and Halpert 1987; Hastenrath, 1994; Del Sole and Shukla, 2002; Gadgil *et al.*, 2005; Kumar *et al.*, 2006). Despite recent progress due to increased spatial and temporal resolution, most numerical climate models have difficulty in capturing the mean monsoon structure and the inter-annual variation (Sperber and Palmer, 1996; Webster *et al.*, 1998; Sperber *et al.*, 2001; Annamalai *et al.*, 2007; Yang *et al.*, 2008) and consequently yield poor seasonal predictions of Asian monsoon strength.

* Correspondence to: W. W. Immerzeel, FutureWater Costerweg 1G, 6702 AA Wageningen, The Netherlands.
E-mail: w.immerzeel@futurewater.nl

Kumar *et al.* (1995) provide a review of methods to forecasts of all India summer monsoon rainfall (AIMSR). They conclude that, irrespective of the type of forecast model used, identification of robust and statistically significant pre-monsoon predictors for AIMSR continues to be of great importance and that many statistics models suffer from significant inter-correlations between different predictors. The Indian Meteorological Department has provided operational forecasts of the AIMSR since 1924 for specific regions in India. For quantitative forecasts, a 16-parameter power regression model is used (Gowariker *et al.*, 1991), which suffers from inter-correlations between the predictors and possibly overfitting (Kumar *et al.*, 1995).

In this study, we choose to combine multiple indicators of imminent monsoon strength as reported in the literature (i.e. ENSO, NAO) with snow cover on the Tibetan Plateau to arrive at seasonal predictions with enhanced skill. To avoid inter-correlation issues, we use a maximum of three predictors per regression model. In particular, we exploit the increasing availability of longer and more reliable time series of remotely sensed high-resolution snow cover data, which have not been used in forecast models. We focus on multiple linear regression prediction of south-west Asian monsoon (SWM) rainfall in the river basins of the Indus, Brahmaputra and Ganges on a pixel basis at a high resolution.

2. Methods

The study area includes the entire catchment areas of the Indus (1,005,786 km²), Ganges (990,316 km²) and Brahmaputra (525,797 km²). During the summer months (June–September), the SWM produces heavy rainfall, specifically in the eastern part of the study area. The monsoon weakens in a western direction. Annual precipitation therefore exhibits an east-to-west gradient ranging from over 2000 mm on the Himalayan foot slopes in the east to less than 300 mm in the arid areas of the Karakoram in the west.

Precipitation data from the tropical rainfall monitoring mission (TRMM) (Kummerow *et al.*, 1998) are used to calculate monsoon precipitation totals from June to September (JJAS) from 1998 to 2008. Here we use the 3B43 product (Huffman *et al.*, 2007), which is a monthly multi-satellite gauge-corrected precipitation with a spatial resolution of 0.25°.

The monthly portion of snow-covered area from April 1998 to September 2008 within the spatial domain 23–41°N and 68–106°E is based on the Normalized Difference Snow Index (Hall *et al.*, 1995) derived from a dataset acquired with the VEGETATION sensor aboard the SPOT 4 and SPOT 5 satellites, similar to the approach of Dankers and de Jong (2004).

Monthly values from 1998 to 2008 for the ENSO indices (Southern Oscillation Index (SOI) (Können *et al.*, 1998) and NINO3 (Rayner *et al.*, 2003)) and the NAO index (Hurrell, 1995) were downloaded from

Table I. Overview of the 16 tested regression models.

Predictor 1	Predictor 2	Predictor 3	$f(-)$	$r(-)$
Snow _{March}	SOI _{winter}	NAO _{winter}	0.47	0.34
Snow _{March}	SOI _{May}	NAO _{winter}	0.46	0.33
Snow _{March}	NINO3 _{winter}	NAO _{winter}	0.48	0.32
Snow _{March}	NINO3 _{May}	NAO _{winter}	0.46	0.33
Snow _{spring}	SOI _{winter}	NAO _{winter}	0.50	0.35
Snow _{spring}	SOI _{May}	NAO _{winter}	0.47	0.31
Snow _{spring}	NINO3 _{winter}	NAO _{winter}	0.50	0.33
Snow _{spring}	NINO3 _{May}	NAO _{winter}	0.49	0.33
Snow _{March}	SOI _{winter}	NAO _{spring}	0.59	0.35
Snow _{March}	SOI _{May}	NAO _{spring}	0.53	0.36
Snow _{March}	NINO3 _{winter}	NAO _{spring}	0.56	0.34
Snow _{March}	NINO3 _{May}	NAO _{spring}	0.55	0.35
Snow _{spring}	SOI _{winter}	NAO _{spring}	0.60	0.35
Snow _{spring}	SOI _{May}	NAO _{spring}	0.58	0.36
Snow _{spring}	NINO3 _{winter}	NAO _{spring}	0.58	0.34
Snow _{spring}	NINO3 _{May}	NAO _{spring}	0.49	0.33

f is the fraction of the total area with $P > 400$ mm year⁻¹ with positive skill and r is the average skill in this area.

the Climate Diagnostic Center of NOAA (accessible at <http://www.cdc.noaa.gov/ClimateIndices/List/>).

We construct linear predictive models for each TRMM pixel by taking JJAS precipitation (P_{JJAS}) as a linear combinations of three different predictors: (1) an ENSO index (either SOI or NINO3), (2) the NAO index and (3) snow cover preceding the monsoon season. For ENSO, the antecedent values for NINO3 and SOI in winter and May are tested. NAO was tested for winter (December–February) and spring (March–May), and snow cover on the Tibetan Plateau for spring and March. Thus, for each pixel for the 11-year time series, 16 models (2 SOI · 2 NINO3 · 2 Snow · 2 NAO = 16) were tested (Table I). If predictors are selected because of their strong correlation with the predictand, this may lead to an apparent skill. However, in our case, each tested model consists of 1 ENSO, 1 snow and 1 NAO predictor and this choice is motivated by pre-established physical considerations and is, as such, less sensitive to screening biases and a resulting apparent skill *cf.* Del Sole and Shukla (2009). The different models are assessed using a rigorous leave-one-out cross-validation procedure. For each model and for each pixel, each year from the time series is iteratively left out. For the remaining 10 years, a model is constructed and the omitted year is predicted using this model. This process is repeated 11 times and the correlation coefficient between the 11 predicted P_{JJAS} and the 11 observed P_{JJAS} is calculated and defined as the predictive skill. The standard deviations of each coefficient of each term in the regression equation are determined on the basis of the 11 repetitions, and used to determine the significance of each term. The models were ranked according to the overall skill within the entire study area for all areas with $P_{JJAS} > 400$ mm year⁻¹, after which the best model (performing best over all pixels >400 mm

year⁻¹) was selected. Pixels with P_{JJAS} less than 400 mm year⁻¹ are not strongly influenced by the monsoon and are therefore not included in the model analysis. This is confirmed by the fact that the correlation between precipitation in areas with $P_{JJAS} < 400$ mm year⁻¹ and $P_{JJAS} > 400$ mm year⁻¹ is very low ($R^2 = 0.0008$). For the best performing model, it was subsequently tested whether inclusion of interaction terms between ENSO, NAO and snow increases model predictive power. For the resulting model, it was then tested if the regression coefficients of the linear model are significant at the 2.5% level (i.e. the 95% confidence interval does not include 0) and, if so, how large is the relative contribution to P_{JJAS} for this variable.

By using a spatial modelling approach, multiplicity is introduced. Therefore, we test if results are not coincidental by testing the field significance (Livezey and Chen, 1983) of the product 'area with positive skill' \times 'average positive skill' (P) that results from using the selected best model. The probability density function of

P is estimated by determining the frequency distribution from a 1000 step Monte Carlo simulation. In each step, the Gaussian noise for each of the three predictors is generated for each pixel. The Gaussian noise is derived on the basis of the distribution of the predictor values. On the basis of the simulated predictor values, the predictive model is constructed for all pixels and the value for P is determined using the same leave-one-out cross-validation procedure. This procedure is repeated 1000 times yielding a frequency distribution of P . Finally, the field significance of the best-performing model is tested by comparing the value of P with the derived frequency distribution.

3. Results

Figure 1(a) shows the large spatial variation in P_{JJAS} . During the SWM, the western end of the monsoon trough is located in the dry convective areas of western India and Pakistan, and the eastern end is locked above

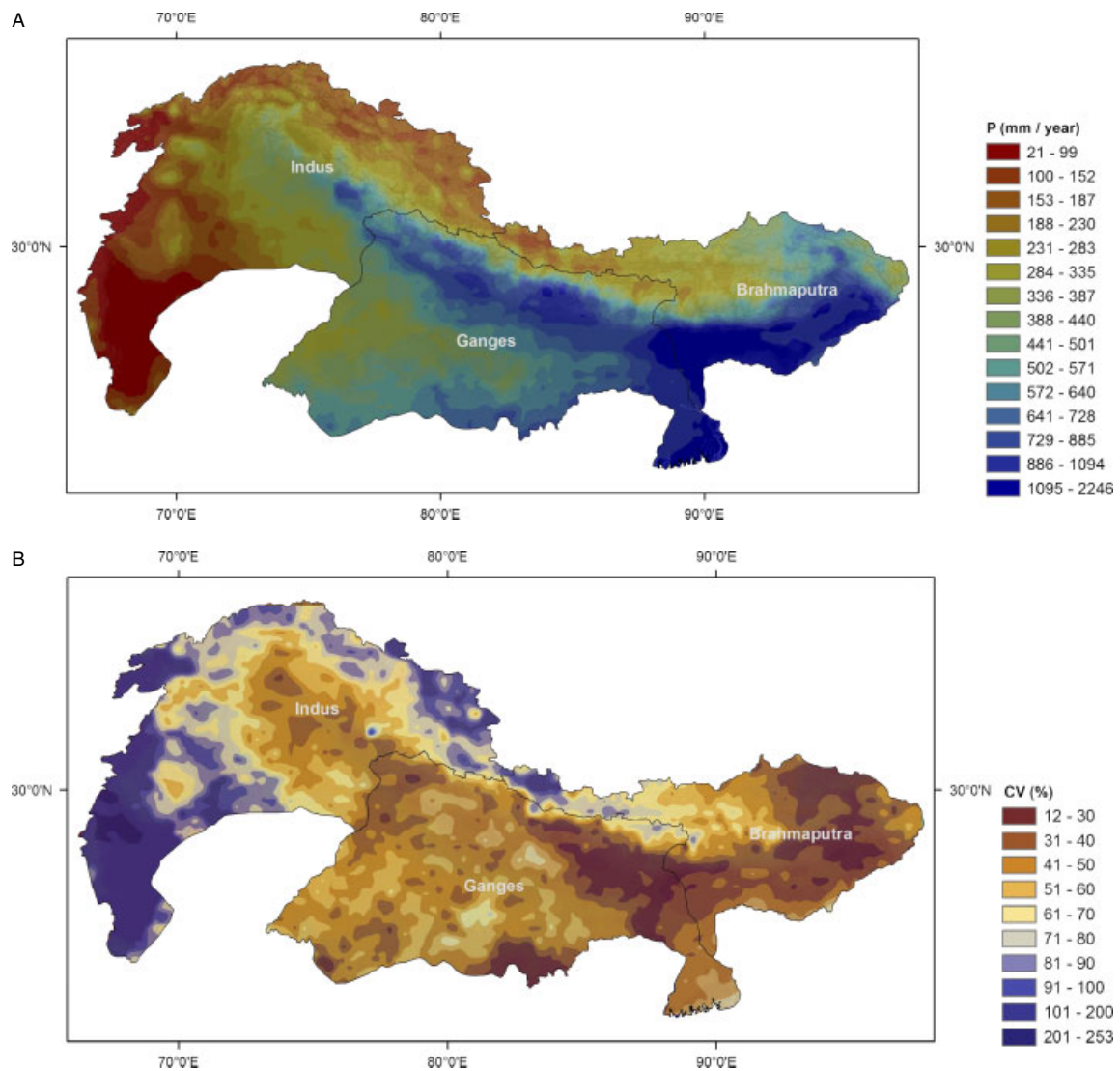


Figure 1. Average P_{JJAS} based on 1998–2008 time series derived from the TRMM 3B43 data product (a) and inter-annual coefficient of variation in JJAS precipitation (b). This figure is available in colour online at wileyonlinelibrary.com/journal/joc

the warm water of the Bay of Bengal. Monsoon lows and depressions develop in the trough, mostly over the northern and central parts of the Bay of Bengal, and these systems subsequently move inland in a north-westerly direction. Once over land, the land surface processes, differential thermal advection and Himalayan relief increase monsoon activity and cause rainfall along the track of the systems. The systems generally weaken in the trough, but some systems move far enough to the west to be reactivated by moisture originating from the Arabian Sea. Figure 1(b) shows that there is considerable inter-annual variation in P_{JJAS} , which is logically much higher in areas with limited rainfall further removed from the Bay of Bengal.

The mean precipitation for all pixels with $P_{JJAS} > 400$ mm was correlated with the previously mentioned predictors to verify if any significant correlations existed. Significant correlations with monsoon precipitation were found with the snow cover in March ($r = -0.68$), snow cover in spring ($r = -0.75$) and SOI in the preceding winter ($r = 0.63$). For the area average, the other predictors were not significant. These results certainly justified the per pixel evaluation of predictive linear models.

The leave-one-out cross validation of the 16 predictive models revealed that the best prediction of P_{JJAS} is achieved by a linear combination of snw_{spring} , SOI_{winter} and NAO_{spring} (Table I). For this case, 60% of the total area with $P_{JJAS} > 400$ mm year⁻¹ has a positive skill with an average of 0.35. This model was then tested to ascertain whether the inclusion of one of the three possible interaction terms ($snw_{spring} \cdot SOI_{winter}$, $snw_{spring} \cdot NAO_{spring}$, $SOI_{winter} \cdot NAO_{spring}$) further increases the model predictive power. This analysis showed that the interaction term $snw_{spring} \cdot NAO_{spring}$ significantly increases the skill, while the other two terms do not show any improvements. The model with the best

overall skill is therefore given by

$$P_{JJAS} = a_1 \cdot snw_{spring} + a_2 \cdot SOI_{winter} + a_3 \cdot NAO_{spring} + a_4 \cdot snw_{spring} \cdot NAO_{spring} + b \quad (1)$$

Where a_1 , a_2 , a_3 and a_4 are coefficients and b is the intercept. For this model, 69% of the total area has a positive skill with an average of 0.37 and a maximum skill of 0.94. In total, 42% of the area with positive skill is significant ($p = 0.1$; $r > 0.42$) and, at $p = 0.05$, the significant area equals 27%. It was found that especially the high rainfall area around the Bay of Bengal can be better predicted by including the interaction term. Evidently, a simultaneous weak phase of NAO, and a low snow cover is a strong predictor of rainfall in this area. Figure 2 shows the spatial distribution of the skill for this best-performing model, and the extensive areas with high P_{JJAS} that can be predicted with reasonable skill. There is a considerable area in the north-western corner of the Ganges basin where the model has no predictive power. This area is also characterized by a low coefficient of variation in P_{JJAS} (Figure 1(b)), i.e. rainfall amounts are very similar each year. Possibly other local orographic processes explain the relatively constant P_{JJAS} in this region. The field significance of the product $P = 0.69 \times 0.37 = 0.255$ was tested and the analysis shows that 0.255 is significant at the 99% confidence level (Figure 3).

Figure 4 shows the observed *versus* the predicted spatial average P_{JJAS} from 1998 to 2008 based on the best model. The correlation coefficient between modelled and observed P_{JJAS} equals 0.75. Notably, the model performs better from 2002 to 2008 than from 1998 to 2002. The variation seems slightly underestimated, which is a common phenomenon in regression modelling. It

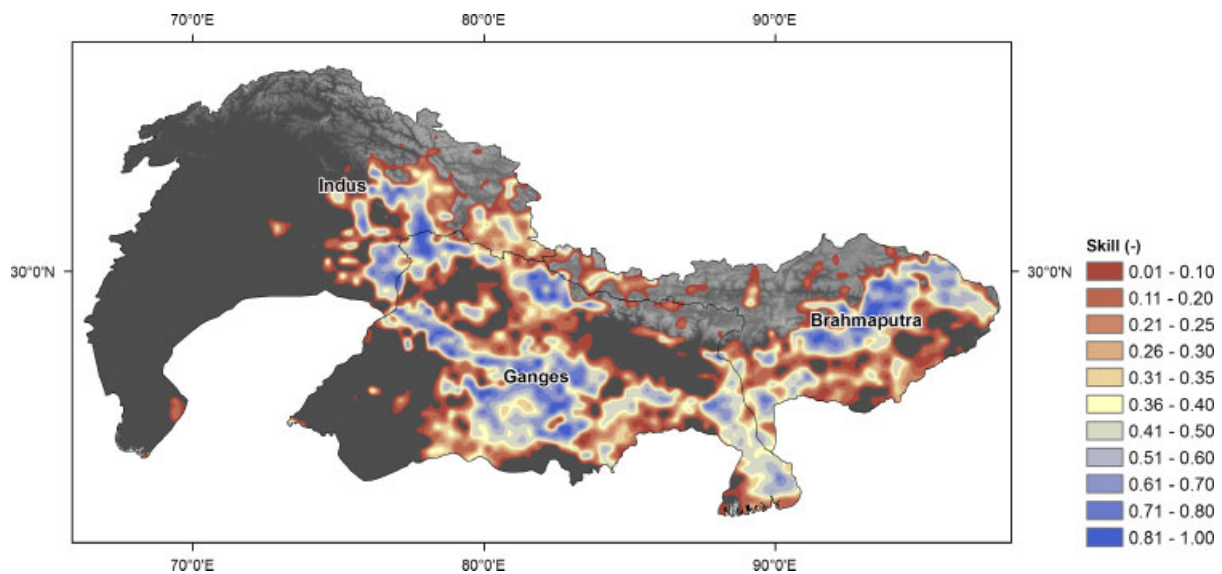


Figure 2. Skill, defined as the correlation coefficient of the leave-one-out cross validation, of the best-performing predictive model. Only areas with a positive skill are shown. This figure is available in colour online at wileyonlinelibrary.com/journal/joc

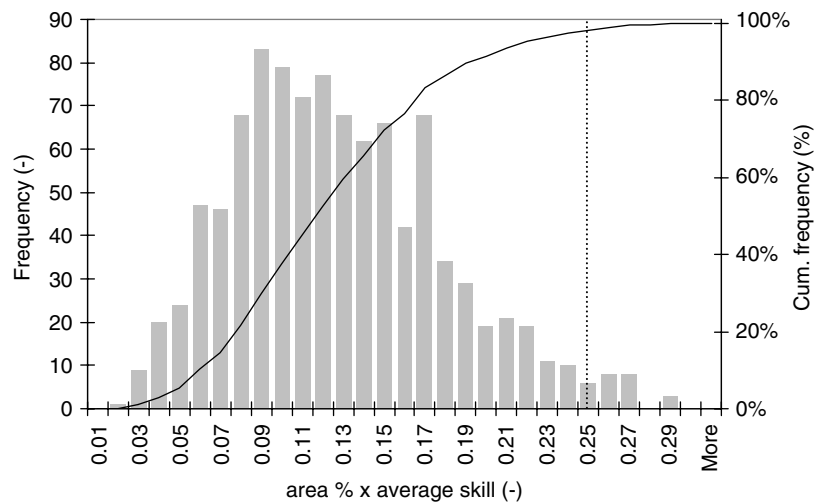


Figure 3. Estimated probability density (bars, left y-axis) and cumulative probability distribution (line, right y-axis) of the metric P (area with positive skill \times average positive skill) in case predictors where completely random. The dotted line shows the value (0.255) of the best performing regression model, which is significant at $p > 0.99$.

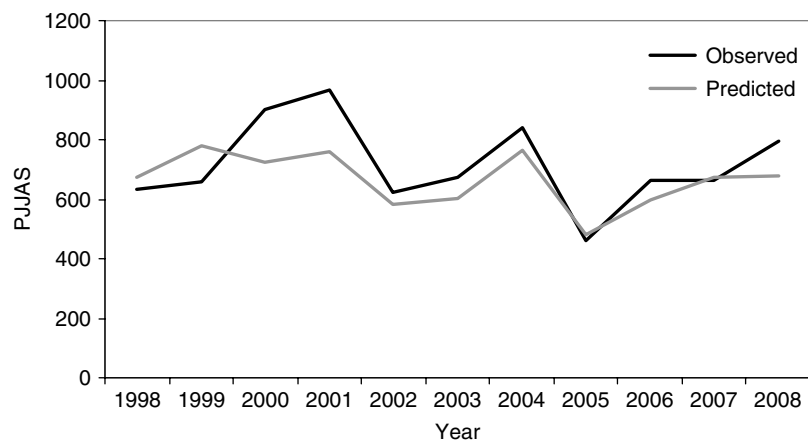


Figure 4. Observed *versus* predicted P_{JJAS} for all pixels with an average $P_{JJAS} > 400 \text{ mm year}^{-1}$.

is, however, worth noting that in 2002 the SPOT 4 satellite was replaced with the SPOT 5 satellite; however, there is currently no evidence that the replacement would improve the estimates.

Using the student t -distribution and the standard deviations of each coefficient of the 11-fold cross validation, it was tested whether the coefficients deviate significantly from zero at the 2.5% significance level. Figure 5 shows the significant areas for all coefficients of Equation (1) and their relative contribution to the prediction of P_{JJAS} . The spring snow cover is most important with the largest significant area and highest weight. Surprisingly, SOI in winter is not a prominent predictor in the model. Although the correlation coefficient was high and significant, it does not add much additional predictive power to the model, except for the area around the Bay of Bengal. The interaction term $\text{snow}_{\text{spring}} \cdot \text{NAO}_{\text{spring}}$ is a prominent predictor in the model, in particular around the Bay of Bengal where P_{JJAS} is highest. The sign of the contribution of snow is negative in almost the entire area. The sign of SOI is positive and the sign of NAO

is negative (in accordance with what is reported in literature) in those areas where the relative contribution is highest, i.e. around the Bay of Bengal. The interaction term, however, has a bi-modal sign. Along the Bay of Bengal, snow and NAO are mutually reinforcing, while on the Ganges plains the signals weaken each other. It is obvious that the areas around the Bay of Bengal and Assam behave differently from the other areas.

Obviously, our predictive model only produces statistical relations between predictor variables and SWM rainfall. Nevertheless, the patterns in Figure 5 deserve a tentative interpretation. The rainfall close to the Bay of Bengal is more related to indices of global circulation modes, such as NAO and ENSO, while more inland, snow cover is most important. This seems to suggest that the strength of the onset of the monsoon closer to the Bay of Bengal is determined by ocean–atmosphere interactions and large-scale circulation, while its inland development is more related to the temperature gradient between ocean and land, which is in turn strongly determined by snow cover on the Tibetan Plateau. The interaction term is more

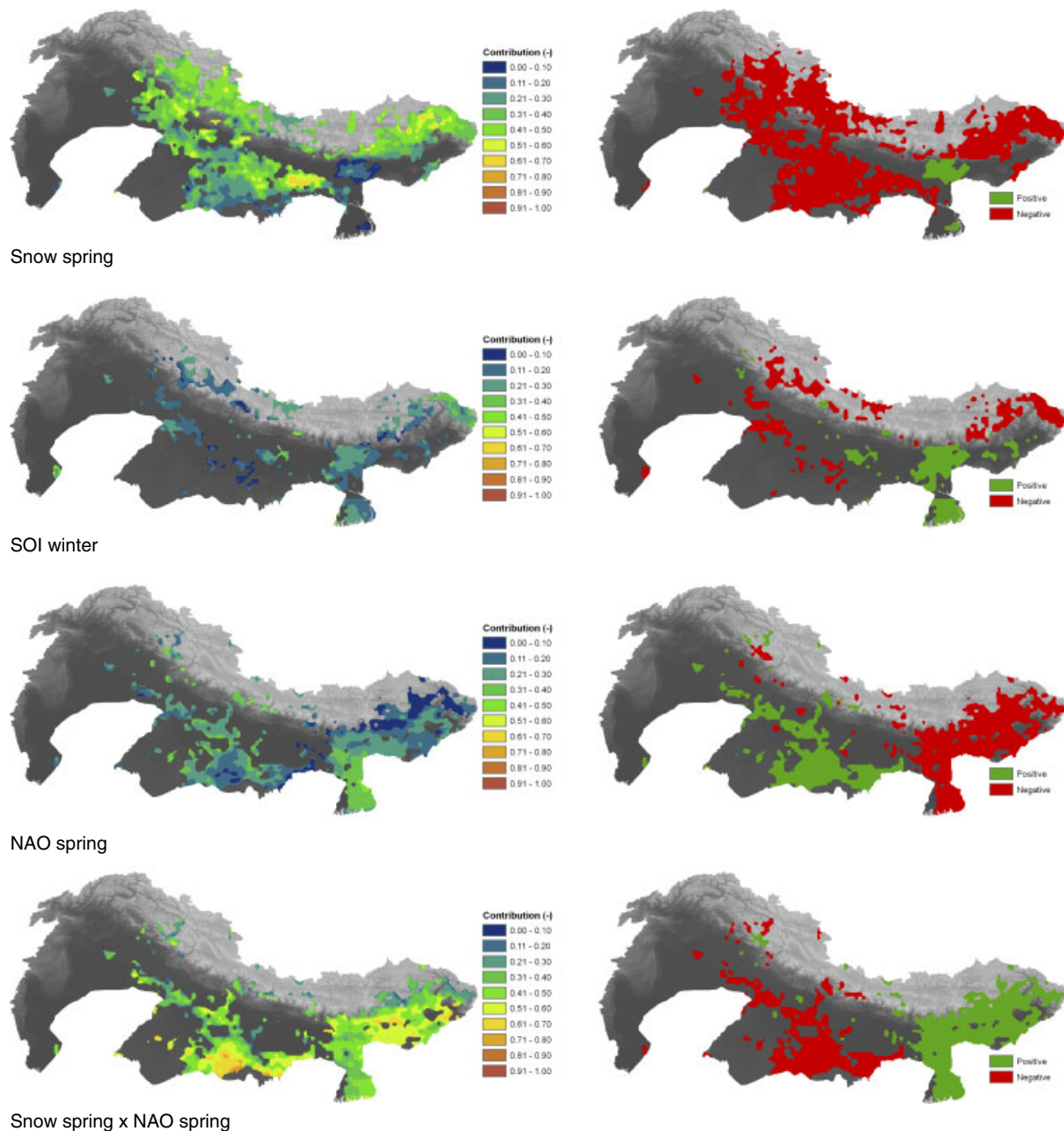


Figure 5. Relative contribution of $\text{snow}_{\text{spring}}$, $\text{SOI}_{\text{winter}}$, $\text{NAO}_{\text{spring}}$ and $\text{snow}_{\text{spring}} \times \text{NAO}_{\text{spring}}$ (left panel) to the predictive model for areas where regression coefficients are significant at the 2.5% confidence level, and respective signs of the contribution of each predictor (right panel). This figure is available in colour online at wileyonlinelibrary.com/journal/joc

difficult to explain. Apparently, the effect of snow cover depends on the NAO phase and vice versa. The small contribution of ENSO is somewhat surprising and may be partly caused by a screening effect of NAO or snow, which possibly interacts with ENSO. This is supported by the correlation coefficients between the different predictors. The correlations between $\text{SOI}_{\text{winter}}$ and $\text{snow}_{\text{spring}}$ (-0.53) and between $\text{SOI}_{\text{winter}}$ and $\text{NAO}_{\text{spring}}$ (-0.41) are relatively high, while the correlation between $\text{snow}_{\text{spring}}$ and $\text{NAO}_{\text{spring}}$ is very low (-0.09). This suggests that the predictive skill of $\text{SOI}_{\text{winter}}$ is in part accounted for by $\text{NAO}_{\text{spring}}$ and $\text{snow}_{\text{spring}}$. However, models with snow and SOI or NAO and SOI perform much worse than models where both snow and NAO are accounted for.

This shows that snow and NAO have a predictive skill of their own and that predictive skill of the SOI by itself is limited.

4. Discussion

The length of the time series used is limited because of the lack of a reliable high-resolution snow cover record on the Tibetan plateau. There is a longer, low-resolution snow cover dataset available that is produced by the National Oceanic and Atmospheric Administration based on visual interpretation of satellite imagery (Robinson *et al.*, 1993; Robinson and Frei, 2000). However, this

dataset is only considered reliable for large regional to hemispheric scale studies, but not over smaller areas, such as the Tibetan plateau.

Previous studies have shown that over prolonged time periods there can be considerable variation in the teleconnection strength between ENSO and Indian Monsoon precipitation, possibly caused by changes in the tropical Atlantic SST (Kucharski *et al.*, 2007), changes in the strength of the Atlantic thermohaline circulation (Lu and Dong, 2008; Lu *et al.*, 2008) or related to sampling variation when analysing the cross-correlation in running means of the limited window size (Oldenborgh and Burgers, 2005); Sterl *et al.*, 2007). Although we show significant and consistent results in our study, these aforementioned studies indicate that, to further confirm and physically substantiate our findings, a longer observation record is desirable.

A number of studies have taken a process-based approach to study the effects of snow cover variation on both the regional and global climate. Barnett *et al.* (1989) used an atmospheric circulation model to perform a number of Eurasian snow cover perturbation experiments. Their main conclusion is that an increased snow cover leads to a subsequent reduction in precipitation over Southeast Asia, which is confirmed by our analysis. Their physical explanation relates to the energy balance and a large proportion of the available energy being consumed by a high albedo, sublimation and evaporative fluxes. Secondly, they argue that after the snow has melted the soil physics and increased soil moisture also results in a decrease in the land–ocean thermal contrast. A study by Dash *et al.* (2006) with a regional climate model also shows a strong response of precipitation to Tibetan snow cover. Their study shows that a prescribed snowpack of 10 cm in April results in a 30% decrease in monsoon rainfall, thus again confirming our findings.

5. Conclusions

We show that the use of remote-sensing time series of precipitation and snow cover, in combination with indices of global atmospheric modes, can predict monsoon precipitation with reasonable skill. Even though the time series is relatively short due to the limited availability of reliable snow cover estimates, a significant inverse relationship is found between spring and March snow cover on the Tibetan plateau and monsoon precipitation. A significant positive relation is also identified between SOI in the preceding winter and monsoon precipitation, confirming earlier findings. The best predictive model of monsoon precipitation is a linear combination of snow cover in spring, SOI in winter, NAO in spring and the interaction term between snow cover in spring and NAO in spring. In total, 69% of the total area has a positive skill and the average positive skill for all areas with $P_{JJAS} > 400$ mm equals 0.37 with an identified field significance of 99%. Snow cover in spring is a strong predictor over large areas of the Ganges plains further

inland, while indices of large-scale circulation modes have a particular predictive power along the Bay of Bengal, where the signs of the predictor contributions are in general in agreement with literature. The physical processes related to these findings require more research, but seem to indicate that the strength of the onset of the monsoon is governed by ocean–atmosphere interactions and large-scale circulation (ENSO, NAO), while the extent to which it travels inland is governed by the thermodynamic conditions above the Tibetan plateau.

Acknowledgements

This study was financially supported by the Netherlands Organisation for Scientific Research (NWO) through a CASIMIR grant (018 003 002) and by the European Commission (Call FP7-ENV-2007-1 Grant nr. 212921) as part of the CEOP- AEGIS project (<http://www.ceop-aegis.org/>) coordinated by the Université de Strasbourg. The authors thank Dr G. J. van Oldenborgh of the Royal Netherlands Meteorological Institute and two anonymous reviewers for their constructive comments.

References

- Annamalai H, Hamilton K, Sperber KR. 2007. The South Asian summer monsoon and its relationship with ENSO in the IPCC AR4 simulations. *Journal of Climate* **20**: 1071–1092.
- Bamzai AS, Shukla J. 1999. Relation between Eurasian snow cover, snow depth, and the Indian summer monsoon: an observational study. *Journal of Climate* **12**: 3117–3132.
- Barnett TP, Dumenil L, Schlese U, Roeckner E, Latif M. 1989. The effect of Eurasian snow cover on regional and global climate variations. *Journal of the Atmospheric Sciences* **46**: 661–685.
- Blanford HF. 1884. On the connexion of the Himalaya snowfall with dry winds and seasons of drought in India. *Proceedings of the Royal Society of London* **37**: 1–23.
- Dankers R, de Jong SM. 2004. Monitoring snow cover dynamics in northern Fennoscandia with SPOT VEGETATION images. *International Journal of Remote Sensing* **25**: 2933–2949.
- Dash SK, Shekhar MS, Singh GP. 2006. Simulation of Indian summer monsoon circulation and rainfall using RegCM3. *Theoretical and Applied Climatology* **86**: 161–172.
- Del Sole T, Shukla J. 2002. Linear prediction of Indian monsoon rainfall. *Journal of Climate* **15**: 3645–3658.
- Del Sole T, Shukla J. 2009. Artificial skill due to predictor screening. *Journal of Climate* **22**: 331–345.
- Gadgil S, Rajeevan M, Nanjundiah R. 2005. Monsoon prediction – why yet another failure. *Current Science* **88**: 1389–1400.
- Gowariker V, Thapliyal V, Kulshrestha SM, Mandal GS, Roy NS, Sikka DR. 1991. A power regression model for long range forecast of southwest monsoon rainfall over India. *Mausam* **42**: 125–130.
- Hahn DG, Shukla J. 1976. An apparent relationship between the Eurasian snow cover and Indian monsoon rainfall. *Journal of the Atmospheric Sciences* **33**: 2461–2462.
- Hall DK, Riggs GA, Salomonson VV. 1995. Development of methods for mapping global snow cover using Moderate Resolution Imaging Spectroradiometer (MODIS) data. *Remote Sensing of Environment* **54**: 127–140.
- Hastenrath S. 1994. *Climate Dynamics of the Tropics: An Updated Edition of Climate and Circulation of the Tropics*. Kluwer Academic Publishers: Norwell, 488.
- Huffman GJ, Adler RF, Bolvin DT, Gu G, Nelkin EJ, Bowman KP. 2007. The TRMM multi-satellite precipitation analysis: Quasi-global, multi-year, combined sensor precipitation estimates at fine scale. *Journal of Hydrometeorology* **8**: 38–55.
- Hurrell JW. 1995. Decadal trends in the North atlantic oscillation and relationships to regional temperature and precipitation. *Science* **269**: 676–679.
- Können GP, Jones PD, Klotfen MH, Allan RJ. 1998. Pre-1866 extensions of the Southern oscillation index using early Indonesian

- and Tahitian meteorological readings. *Journal of Climate* **11**: 2325–2339.
- Kumar KK, Soman MK, Kumar KR. 1995. Seasonal forecasting of Indian summer monsoon rainfall: a review. *Weather* **50**: 449–467.
- Kumar K, Rajagopalan B, Cane MA. 1999. On the weakening relationship between the Indian monsoon and ENSO. *Science* **284**: 2156–2159.
- Kumar KK, Rajagopalan B, Hoerling M, Bates G, Cane MA. 2006. Unraveling the mystery of Indian monsoon failure during El Niño. *Science* **314**: 115–119.
- Kummerow C, Barnes W, Kozu T, Shiue J, Simpson J. 1998. The Tropical Rainfall Measuring Mission (TRMM) sensor package. *Journal of Atmospheric and Oceanic Technology* **15**: 809–817.
- Kucharski F, Bracco A, Yoo JH, Molteni F. 2007. Low-frequency variability of the Indian monsoon-ENSO relationship and the tropical Atlantic: the “Weakening” of the 1980s and 1990s. *Journal of Climate* **20**: 4255–4266.
- Li C, Yanai M. 1996. The onset and interannual variability of the Asian summer monsoon in relation to land-sea thermal contrast. *Journal of Climate* **9**: 358–375.
- Liu X, Yanai M. 2001. Relationship between the Indian monsoon rainfall and the tropospheric temperature over the Eurasian continent. *Quarterly Journal of the Royal Meteorological Society* **127**: 909–937.
- Livezey R, Chen W. 1983. Statistical field significance and its determination by Monte Carlo techniques. *Monthly Weather Review* **111**: 46–59.
- Lu R-Y, Dong B-W. 2008. Response of the Asian summer monsoon to a weakening of Atlantic thermohaline circulation. *Advances in Atmospheric Sciences* **25**: 723–736.
- Lu R-Y, Chen W, Dong B-W. 2008. How does a weakened Atlantic thermohaline circulation lead to an intensification of the ENSO-south Asian summer monsoon interaction? *Geophysical Research Letters* **35**: L08706.
- Oldenborgh GJvan, Burgers G. 2005. Searching for decadal variations in ENSO precipitation teleconnections. *Geophysical Research Letters* **32**: L15701.
- Rayner NA, Parker DE, Horton EB, Folland CK, Alexander LV, Rowell DP, Kent EC, Kaplan A. 2003. Global analyses of sea surface temperature, sea ice, and night marine air temperature since the late nineteenth century. *Journal of Geophysical Research* **108**(D14): 4407. DOI:10.1029/2002JD002670.
- Robinson DA, Dewey DF, Heim R Jr. 1993. Global snow cover monitoring: an update. *Bulletin of the American Meteorological Society* **74**: 1689–1696.
- Robinson DA, Frei A. 2000. Seasonal variability of northern hemisphere snow extent using visible satellite data. *The Professional Geographer* **51**: 307–314.
- Robock A, Mu M, Vinnikov K, Robinson D. 2003. Land surface conditions over Eurasia and Indian summer monsoon rainfall. *Journal of Geophysical Research* **108**(D4): 4131. DOI:10.1029/2002JD002286.
- Ropelewski CF, Halpert MS. 1987. Global and regional scale precipitation patterns associated with the El Niño/southern oscillation. *Monthly Weather Review* **115**: 1606–1626.
- Shaman J, Cane M, Kaplan A. 2005. The relationship between Tibetan snow depth, ENSO, river discharge and the monsoon of Bangladesh. *International Journal of Remote Sensing* **26**: 3735–3748. DOI: 10.1080/01431160500185599.
- Shaman J, Tziperman E. 2005. The effects of ENSO on Tibetan Plateau Snow depth: a stationary wave teleconnection mechanism and implication for the south Asian monsoons. *Journal of Climate* **18**: 2067–2079.
- Shukla J, Paolino DA. 1983. The southern oscillation and long range forecasting of the summer monsoon over India. *Monthly Weather Review* **111**: 1830–1837.
- Sperber KR, Brankovic C, Déqué M, Frederiksen CS, Graham R, Kitoh A, Kobayashi C, Palmer T, Puri K, Tennant W, Volodin E. 2001. Dynamical seasonal predictability of the Asian summer monsoon. *Monthly Weather Review* **129**: 2226–2248.
- Sperber K, Palmer T. 1996. Interannual tropical rainfall variability in general circulation model simulations associated with the atmospheric model intercomparison project. *Journal of Climate* **9**: 2727–2750.
- Sterl A, van Oldenborgh GJ, Hazeleger W, Burgers G. 2007. On the robustness of ENSO teleconnections. *Climate Dynamics* **29**: 469–485.
- Yang S, Lau KM, Yoo SH, Kinter JL, Miyakoda K, Ho CH. 2004. Upstream subtropical signals preceding the Asian summer monsoon circulation. *Journal of Climate* **17**: 4213–4229.
- Yang S, Zhang Z, Kousky VE, Higgins RW, Yoo S-H, Liang J, Fan Y. 2008. Simulations and seasonal prediction of the Asian summer monsoon in the NCEP climate forecast system. *Journal of Climate* **21**: 3755–3775.
- Wang B. 2006. Preface. In *The Asian Monsoon*, Wang N (ed). Springer and Praxis: Chichester.
- Webster P, Magaña V, Palmer T, Shukla J, Tomas R, Yanai M, Yasunari T. 1998. Monsoons: processes, predictability, and the prospects for prediction. *Journal of Geophysical Research* **103**(C7): 14451–14510.